Available online at www.sciencedirect.com

ScienceDirect

Physics Procedia 10 (2010) 17–21

Physics Procedia

www.elsevier.com/locate/procedia

3rd International Symposium on Shape Memory Materials for Smart Systems

Shape memory characteristics of powder metallurgy processed $Ti_{50}Ni_{50}$ alloy

Yeon-wook Kim* and Kyung-su Jeon

Department of Advanced Materials Engineering, Keimyung University
1000 Shindang-dong, Dalseo-gu, Daegu, 704-701, South Korea

Abstract

$Ti_{50}Ni_{50}$ shape memory alloy powders were prepared by inert gas atomization and the powders were consolidated by spark plasma sintering (SPS) to fabricated dense bulk samples. Martensitic transformation temperatures and microstructures of the as-atomized powders and the consolidated disks were investigated. DSC and XRD analysis showed that the B2-B19' martensitic transformation occurred in the powders and the disks. The martensitic transformation start temperature (M_s) of the powders was 22.9 ℃. However, the M_s of the SPS disk was 65.9 ℃. It is considered that this increase in transformation temperature is ascribed to the microstructural change during SPS processing.

Keywords: Shape memory alloys, Ti-Ni powders, Spark plasma sintering, Martenstic transformation

1. Introduction

Ti-Ni based alloys are the most successful shape memory alloys due to their unique functional properties, which make them highly attractive for many applications including thermal and mechanical actuators and biomedical applications [1,2]. Their additional distinctive characteristics such as good ductility, high corrosion and fatigue resistance besides great damping capability and considerable strength and toughness have led to various commercial applications in different industrial fields, among which the medical applications dominate [3]. This results from not only the above mentioned unique and superior properties of TiNi alloys but also their proven biocompatibility, which is essential for biomedical applications [4].

Powder metallurgy is a promising method for production of near-net-shape components of TiNi alloys because expensive thermomechanical treatments, machining and associated materials losses can be avoided or minimized [5]. Furthermore, TiNi alloys in porous form have attracted an additional interest as biomaterials for implantation since the introduction of pores into the bulk material provides ingrowth of living tissues and firm fixation in addition to reducing the alloy density [6]. Recently, shape memory alloys has been also studied as damping materials, and it is

* Corresponding author. Tel.: +82-53-580-5547; fax: +82-53-580-5547
E-mail address: ywk@kmu.ac.kr.

1875-3892 © 2010 Published by Elsevier Ltd Open access under CC BY-NC-ND license.
doi:10.1016/j.phpro.2010.11.068

considered that TiNi bulk specimens are especially suitable for damping materials [7]. Hence consolidation of powders is appropriate for preparing biomaterials and high damping materials. Pure elemental Ti and Ni powders are often used as raw materials for the preparation of porous TiNi alloys through self-propagating high temperature synthesis [8]. Generally, the alloy is formed in solid state via inter diffusion reactions between Ti and Ni powders. The porous TiNi alloys synthesized by hot isostatic pressing and conventional sintering method exhibit martensitic transformations, but often with reduced latent heat, suggesting incomplete formation of the TiNi B2 phase. In fact, all TiNi alloys synthesized via solid-state reaction processes were found to contain considerable amounts of undesired secondary intermetallics such as Ti_2Ni and $TiNi_3$ [9] and were also observed to result in non-spherical pores, non-homogeneous pore distribution in the structure and sharp pore edges that act as stress risers. Then the presence of Ti_2Ni and $TiNi_3$ in the TiNi matrix may cause a degradation of the shape memory properties and mechanical properties.

One way to overcome these problems is to synthesize the near-net-shape TiNi alloys bulks from the alloy powders. Therefore, it is necessary to fabricate homogeneous TiNi powders and to examine their martensitic transformation behavior and microstructures. This study investigated the fabrication of $Ti_{50}Ni_{50}$ powders through gas atomization, and the martensitic transformation temperatures and microstructures of the rapidly solidified powders were examined as a function of powder size. TiNi alloy bulks were also fabricated in the form of cylindrical disks from the gas atomized powders by spark plasma sintering and their martensitic transformation behaviors were compared with those of the as-atomized powders.

2. Experimental Procedure

Ti-Ni alloy ingots with nominal composition of 50Ni-50Ni (at.%) were prepared by melting high purity nickel and sponge titanium in a high frequency induction furnace under vacuum. TiNi shape memory alloy powders were prepared by gas atomization unit in high vacuum atmosphere. Prior to gas atomization, the oxide layer on the surface of the ingots was removed by grinding to minimize impurity contents. Powders were synthesized by melting the ingots (about 800g) in a graphite crucible at 1450 ℃, and then pouring it through a graphite melt delivery nozzle of 7 mm diameter at the bottom into a confined Ar gas atomizer operating at a pressure of 1.2 MPa. The melt flow rate, estimated from the operating time and weight of the atomized melt, was about 4 kg/min. The gas flow rate, calculated from the gas consumption rate, was about 1.0 Nm^3/min. The size distribution of the powder was measured by conventional mechanical sieving, and sieved powders with the specific size range of 0 to 200 μm were chosen for this investigation.

A dense TiNi disk was prepared from the as-atomized powder by spark plasma sintering (SPS). Ten grams of the powder to be consolidated was poured into a cylindrical graphite die (20 mm in inside diameter and 50 mm in outside diameter). The die was then placed in the vacuum chamber of a SPS apparatus and the system was evacuated. This step was followed by the application of a mechanical pressure through the plungers. The temperature increased to 1100 ℃ directly at a rate of 50℃/min. The powder was maintained at the desired temperature for 20 min. During the entire SPS process, a mechanical pressure of 10 MPa was maintained, and an electrical current of 700 A was applied. Finally these sintered samples were heat-treated for 20 min at 800 ℃, and then quenched in water. Cylindrical disks (20 mm in diameter and 0.5 mm in thickness) were fabricated. The microstructures of as-atomized powder and the consolidated samples were examined after etching in a solution of H_2O:HCl:H_2O_2 (3:2:1). The crystal structure of the powder was analyzed by X-ray diffraction (XRD) using CuK_α radiation. For the study of martensitic transformation behaviors of the as-atomized powder and the consolidated disks, differential scanning calorimetry (DSC) measurements were performed at heating and cooling rate of 10℃ /min using TA Instrument DSC-2010.

3. Results and Discussion

A series of sieves was used to obtain particular powder distribution. About 370g of the atomized powders was smaller than 300 μm. In this study, powders less than 200 μm were examined because the shape of powders larger than 200 μm is irregular or needle-like. Fig. 1 shows typical SEM images of the gas-atomized $Ni_{50}Ni_{50}$ powders. Evaluation of powder microstructures is based on SEM examination of the surface as shown in Fig. 1(a) and the polished and etched powder cross sections as shown in Fig. 1(b). The surface of gas-atomized powders is ideally

smooth and spherical. One of the characteristic features of the gas-atomized powders is satelliting as shown in Fig. 1(a), especially when finer powders are produced. This is the decoration of the lager particles by attached small particles. This is believed to be caused by the circulation of gas within the atomizing chamber that lifts finer particles back into the spray plume, where they collide with larger, still partly molten particles. The powders show cellular morphology as seen in Fig. 1(b) and clearly contain porosities which are located in intercellular regions. Most metals form shrinkage porosity during solidification that is atomically less dense than the melt. This solidification shrinkage may occur at the cell boundaries where the solidification fronts meet together during the final stage of solidification.

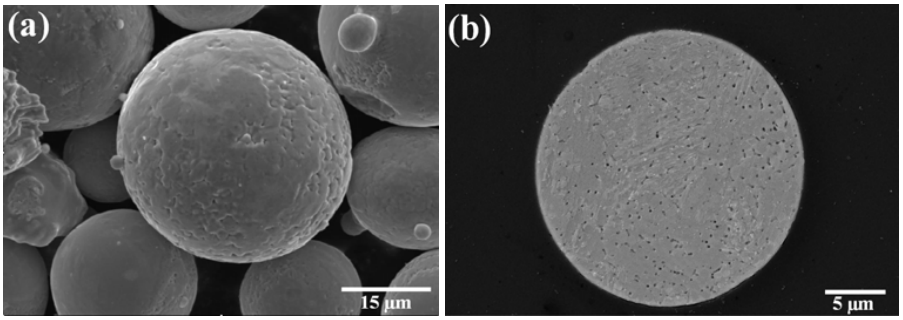

Fig. 1 SEM Micrographs of (a) the typical surface and (b) the cross sections of gas-atomized powders.

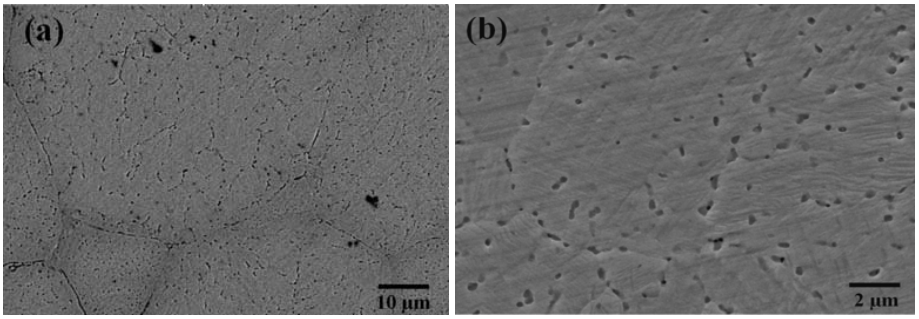

Fig. 2 SEM Micrographs of the SPS consolidated sample.

Fig. 2 shows typical SEM images of a consolidated TiNi sample. High-density structure was obtained in the sample by spark plasma sintering as shown in Fig. 2(a). It could be observed that small particles were filled in the interspaces among the bigger particles. When the microstructure of the consolidated samples was observed by high magnification field-emitting SEM, it was found that there was high population of very small pores. They were shrinkage pores in the as-atomized particles. However, these pores were not removed or deformed during SPS.

DSC curves of as-atomized TiNi powder and the consolidated samples are presented in Fig. 3. It is seen that all DSC curves show one exothermic peak on cooling and one endothermic peak on heating. In order to explain the transformation behavior of $Ni_{50}Ni_{50}$ alloy in the DSC measurement of Fig. 2(a), XRD experiments were carried out for the consolidated sample. Fig. 4 shows the analytical results of XRD patterns as a function of the temperature. On cooling the sample, at 60 ℃, the diffraction peak of the B19' (monoclinic) martensite starts to appear, as shown in

Fig. 4(a). On further cooling, at 40 ℃, the intensities of the diffraction peaks of the B2 (cubic) parent phase decrease, while those of the B19' martensite increase. On further cooling, at 0 ℃, the diffraction peaks of the B2 parent phase disappear. On heating the sample, at 30 ℃, the diffraction peaks of the B2 parent phase start to appear as shown in Fig. 4(b). On further heating, at 80 ℃, the intensity of a diffraction peak of the B19' martensite phase decreases, while those of the B2 phase increase. On further heating, at 110 ℃, the diffraction peak of the B19' phase disappears. Therefore, the exothermic DSC peak on cooling in the curve of Fig. 3(b) is attributed the B2→B19' martensitic transformation and the endothermic peak on heating is ascribed to the B19'→B2 reverse transformation. This one-step transformation was also found in the as-atomized powders. From Fig. 3 and 4, it is concluded that the one-step B2-B19' transformation occurs in the rapidly solidified $Ti_{50}Ni_{50}$ powders and the consolidated sample. The M_s (B2→B19' martensitic transformation start temperature) and the A_f (B19'→B2 austenite transformation finish temperature) of the as-atomized $Ti_{50}Ni_{50}$ powder are 22.9 ℃ and 52.3 ℃, respectively.

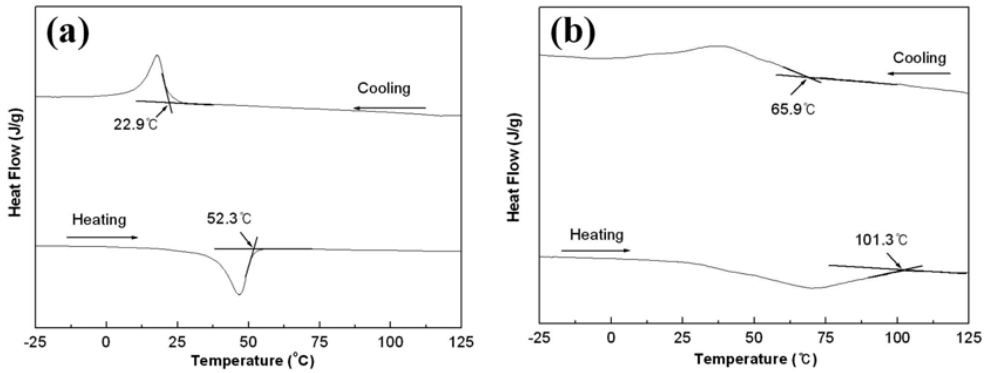

Fig. 3 DSC curves of (a) the as-atomized powders and (b) the SPS consolidated sample.

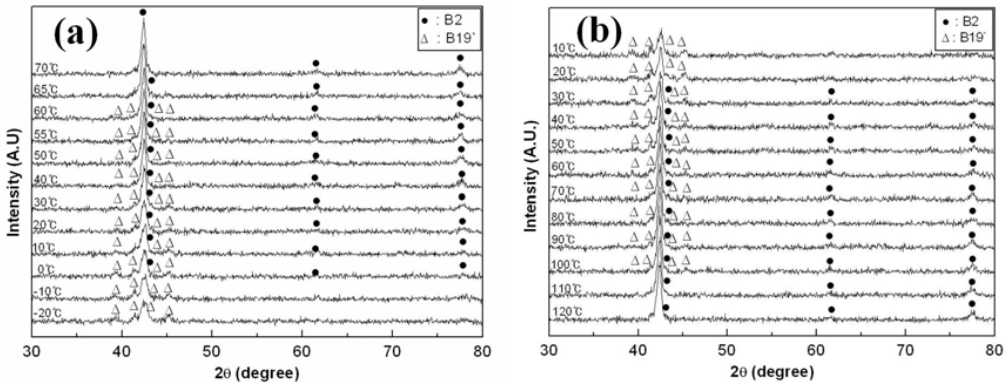

Fig. 4 XRD patterns of the SPS consolidated sample (a) on cooling and (b) on heating.

In the consolidated sample, the M_s and A_f are 65.9 ℃ and 101.3 ℃, respectively, as shown in Fig 3. (b). Transformation temperatures of the consolidated samples are clearly higher than those of as-atomized powders and

the peaks are relatively broad. Because martensitic transformation behavior sensitively depends on alloy composition in Ti-Ni shape memory alloys [10], the chemical compositions of the as-atomized powder and the consolidated sample were analyzed by EDS. It was found that Ti-content was 50.2±0.07 at% and chemical composition distribution was very homogeneous in the powder. In the consolidated sample, however, relatively inhomogeneous chemical composition distribution is observed and Ti-content was 50.6±0.28 at%. It is found that Ti-content of the consolidated sample is higher than that of the powder. The increase of transformation temperatures in the consolidated sample is ascribed to Ti-rich matrix which was formed during SPS process. Since transformation temperature depends largely on chemical composition, the wide DSC peaks of the consolidated sample would be ascribed to the inhomogeneous chemical composition distribution.

4. Conclusion

$Ti_{50}Ni_{50}$ shape memory powders were produced by means of gas atomization under a vacuum atmosphere. Dense alloy samples were fabricated from the as-atomized alloy powder by spark plasma sintering. One-step martensitic transformation of B2-B19' is observed during cooling and heating in the powder and the consolidated sample. The martensitic transformation start temperature (M_s) and the austenite transformation finish temperature (A_f) of the as-atomized powder are 22.9 ℃ and 52.3 ℃, respectively. The M_s and A_f of the consolidated samples are 65.9 ℃ and 101.3 ℃, respectively. The increase of transformation temperatures in the consolidated samples is ascribed to decomposition and shrinkage related stresses during the spark plasma sintering process.

5. Acknowledgement

This work was supported by the Korea Research Foundation Grant funded by the Korean Government (KRF-2008-313-D00419).

References

[1] K. Otsuka, X.B. Ren, Intermetallics 7 (1999) 511.
[2] J. Van Humbeeck, Mater. Sci. Eng. A 273-275 (1999) 134.
[3] K. Otsuka, X.B. Ren, Prog. Mater. Sci. 50 (2005) 511.
[4] O. Prymak, D. Bogdanski, M. Köller, S.A. Esenwein, G. Muhr, F. Bekmann, T. Donath, M. Assad, M. Epple, Biomaterial, 26 (2005) 5801.
[5] S.K. Wu, H.C. Lin, C.C. Chen, Mater. Lett. 40 (1999) 27.
[6] V.I. Itin, V.E. Gjunter, S.A. Shabalovskaya, R.L.C. Sachdeva, Mater. Characterization 32 (1994) 179.
[7] Y. Zhao, M. Taya, Y Kang, A. Kawasaki, Acta Mater. 53 (2005) 337-343.
[8] S.L. Wu, X.M. Liu, P.K. Chu, C.Y. Chung, C.L. Chu, K.W.K. Yeung, J. Alloys Compd. 449 (2008) 139.
[9] J. Laeng, Z. Xiu, X. Xu, X. Sun, H. Ru, Y. Liu, Phys. Scipta, T129 (2007) 250.
[10] J. Mentz, J. Frenzel, M. Wagner, K. Newking, G. Eggeler, H.P.Buchkremer, D. Stover, Mater. Sci. Eng. A 491 (2008) 270.